Catalysis Communications 60 (2015) 50–54

Contents lists available at ScienceDirect

Catalysis Communications

journal homepage: www.elsevier.com/locate/catcom

Short communication

Preparation of Ni–W–P–B amorphous catalyst for the hydrodeoxygenation of *p*-cresol

Weiyan Wang, Sijun Yang, Zhiqiang Qiao, Pengli Liu, Kui Wu, Yunquan Yang *

School of Chemical Engineering, Xiangtan University, Xiangtan City, Hunan 411105, PR China

ARTICLE INFO

Article history:
Received 2 August 2014
Received in revised form 18 November 2014
Accepted 20 November 2014
Available online 22 November 2014

Keywords:
Hydrodeoxygenation
Ni–W–P–B
Catalyst preparation
p-Cresol
Bio-oil

ABSTRACT

Ni–W–P–B amorphous catalysts were prepared by a modified chemical reduction method. The formation of a complex between Ni^{2+} and $NH_3 \cdot H_2O$ inhibited the reaction rate of Ni^{2+} with BH_4^-, leading to a high Ni^0 content on the catalyst surface. The effects of Ni/W molar ratio on the catalytic activity in the hydrodeoxygenation (HDO) of *p*-cresol were studied. The deoxygenation degree reached to 100% with a toluene selectivity of 5.1% at 498 K. The HDO reaction temperature and aromatic yield decreased obviously. Some of toluene was produced from the dehydrogenation of 3-methylcyclohexene. Ni–W–P–B exhibited high HDO activity and dehydrogenation activity.

1. Introduction

The increase of energy consumption and emissions of greenhouse gases in the utilization of fossil fuels have aroused a wide research in the exploration of a sustainable and renewable replacement for petroleum based fuel [1–3]. Bio-oil, a liquid fraction derived from the pyrolysis of lignocellulosic materials, is considered as a significant candidate for fuel due to its CO_2-neutral and SO_X-free emission upon combustion [4]. However, this bio-oil contains high oxygen content, leading to some disadvantages such as low heating value, chemical instability and immiscibility with fossil fuels, which prevents its direct utilization as a transportation fuel. The main challenge for upgrading bio-oil to liquid hydrocarbons is to remove the oxygenated functionalities effectively. One of the most efficient technologies is catalytic hydrodeoxygenation (HDO).

Until now, many studies regarding HDO have been carried out by using model compounds [5–13]. Among these oxygenated functionalities in the bio-oil, phenolic hydroxyl oxygen is considered as the most difficult one to remove because the direct scission of this C–O bond requires the highest activation energy [4], leading to a high reaction temperature for achieving the high deoxygenation degree. For example, K. J. Smith et al. [14] had studied the HDO of phenols on MoS_2 with different morphologies and found that the highest conversion of *p*-cresol was 75% after 7 h reaction at 623 K and 2.8 MPa of H_2. Adopting the synergistic effect between W and Mo and the promoter effect, Wang et al. [15] had studied the HDO of *p*-cresol on Ni–Mo–W–S and obtained a conversion of 97.8% after 5 h reaction at 573 K and 3.0 MPa of H_2. Yang et al. [16] had reported that the conversion of phenol on CoMoP/MgO was 89.8% with a benzene selectivity of 64% at 723 K and 5 MPa of H_2. Our previous study [17] had found that *p*-cresol conversion on Ni–P catalyst was only 85.0% after 10 h reaction at 623 K and 4.0 MPa of H_2.

The HDO of phenols usually proceeds with two parallel routes: direct hydrogenolysis (DDO) yielding aromatics and hydrogenation–dehydration producing cycloalkanes (HYD). According to the quality standards for clean fuel and World Fuel Oil Regulation IV, benzene and aromatic contents in gasoline were strictly limited because of their harmfulness for human health. The latter one avoids the direct scission of C–O σ-bond in phenolic hydroxyl, which can decrease the HDO reaction temperature but require a high hydrogenation activity for the catalyst. We had reported that Ni–W–B amorphous catalyst exhibited high HDO activity and the activity depended on the numbers of metal Ni^0 sites and Brönsted acid sites [18]. However, Ni^0/Ni on the surface of Ni–W–B catalyst was only 0.27 [18], suggesting that its HDO activity, especially for hydrogenation, could be further improved. Li et al. [19] had reported that adding P into Ni–B catalyst enhanced its hydrogenation activity. In fact, Ni^{2+} can react with NH_4^+ to produce a complex, which might decrease the reaction rate of Ni^{2+} with BH_4^- after forming the complex and then promote the reduction of Ni^{2+} to Ni^0. Therefore, aiming to prepare a HDO catalyst with high activity, we used $Ni(NO_3)_2$, Na_2WO_4, $NH_3 \cdot H_2O$, NaH_2PO_2 and $NaBH_4$ as raw materials to synthesize Ni–W–P–B amorphous catalysts and studied their activity by taking the HDO of *p*-cresol as a probe.

* Corresponding author.
E-mail address: yangyunquan@xtu.edu.cn (Y. Yang).

http://dx.doi.org/10.1016/j.catcom.2014.11.023
1566-7367/

2. Experimental

2.1. Catalyst preparation

Ni–W–P–B amorphous catalysts were prepared by the following steps. $NiSO_4 \cdot 6H_2O$ (1.57 g) and NaH_2PO_2 (1.0 g) were dissolved in 25 mL H_2O solution, and then $NH_3 \cdot H_2O$ (25 wt.%, 1.6 g) and $Na_2WO_4 \cdot 2H_2O$ were added into the above solution following placed in a 250 mL three-necked flask. A 20 mL $NaBH_4$ (1.0 g) aqueous solution was added dropwise to the three-necked flask with vigorous agitation at 273 K. The resulting black precipitate was washed with water and ethanol. Finally, the sample was dried under vacuum at 323 K for 4 h and was donated as Ni–W-X, where X represented the Ni/W molar ratio in the initial solution.

2.2. Catalyst characterization

Specific surface area was measured by a Quantachrome's NOVA-2100e Surface Area instrument by physisorption of nitrogen at 77 K. The prepared samples were dehydrated at 460 K using vacuum degassing for 12 h before analysis. X-ray diffraction (XRD) test was carried on a D/max 2550 18 kW Rotating anode X-ray Diffractometer with Cu Kα ($\lambda = 1.5418$ Å) radiation (40 kV, 300 mA). The surface composition and surface electronic state were analyzed by X-ray Photoelectron Spectroscopy (XPS) using Kratos Axis Ultra DLD instrument.

2.3. Catalyst activity measurement

The catalyst activity tests were carried out in a 300-mL sealed autoclave. The fresh catalyst (0.2 g, particle size ≤75 μm), *p*-cresol (13.51 g) and dodecane (86.49 g) were placed into the autoclave. Air in the autoclave was evacuated by pressurization–depressurization cycles with nitrogen and subsequently with hydrogen. The mixture was heated at 10 K/min to 298 K, then pressurized with hydrogen to 4.0 MPa, and stabilized the stirring speed at 900 rpm. During the reaction, the pressure, stirrer speed, and temperature were kept constant. Liquid samples were withdrawn from the reactor and analyzed by Agilent 6890/5973N GC–MS. To separate the reaction products, the temperature in the GC oven was heated from 313 K to 358 K with the ramp of 20 K/min, held at 358 K for 4.0 min, then heated to 473 K at a rate of 20 K/min and kept at 473 K for 5.0 min. The carbon balance in the sample for each of experiment was better than 95 ± 3%. External and internal mass transfer limitations could be neglected because of the small catalyst particle size and high stirring speed. The amounts of *p*-cresol and products were analyzed by Agilent 7890 gas chromatography using a flame ionization detector (FID) with a 30 m AT-5 capillary column. The deoxygenation degree (DD) for each experiment was calculated as follows:

$$\text{Deoxygenation degree (DD, wt.\%)} = \left(1 - \frac{\text{oxygen content in the final organic compounds}}{\text{total oxygen content in the initial material}}\right) \times 100\%.$$

3. Results and discussion

3.1. Characterization of Ni–W–P–B catalysts

Fig. 1 shows the XP spectra of Ni 2p, B 1s, P 2p and W 4f levels of Ni–W–P–B, samples. Each of the spectra was deconvoluted, and the relative content of each state was calculated based on the corresponding peak area. It had reported that the standard binding energy of elemental Ni, B, P and W was 853.0, 187.0, 130.4 and 31.0 eV [19,20], respectively, revealing that all species in the prepared catalysts were present in both oxidized state and elemental state. Two strong peaks at 852.4 and 855.8 eV and one weak peak at 860.4 eV appeared in Fig. 1a, corresponding to metal Ni, NiO and $Ni(OH)_2$ [20,21], respectively. All B 1s spectrums displayed two peaks at 187.8 and 192.1 eV. The former one was attributed to elemental B, while the latter one was attributed to B^{3+} [20,21]. In the Fig. 1c, the peaks around 129.5 and 133.4 eV were assigned to elemental phosphorus with metal nickel and oxidized phosphorus, respectively. In comparison with the standard binding energies of pure Ni, B and P, a positive shift of the elemental B and a negative shift of the elemental Ni and P were observed in all the as-prepared samples. These observations implied that the elemental B donated partial electrons to the metal Ni and the phosphorus accepted electrons from the nickel metal, which was in good accordance with previous investigations [22,23]. The peaks around 31.4 eV and 33.4 eV in Fig. 1d were attributed to W^0, while the peaks around 35.6 eV and 37.7 eV were attributed to WO_3 [20]. The appearance of W^0 suggested that some W^{6+} was reduced to metal W.

The surface compositions of Ni–W-2, Ni–W-1, Ni–W-0.5 and Ni–W-0.33 samples are summarized and listed in Table 1. With the decrease of Ni/W mole ratio in the raw material, Ni/W mole ratio on the catalyst surface was decreased from 1:0.22 for Ni–W-2 to 1:4.36 for Ni–W-0.33. This resulted from the reaction of Ni^{2+} with NH_4^-. The amount of Ni^{2+} in the reaction system decreased gradually, but the total of NH_4^- kept constant. After forming the complex, the remained NH_4^- was increased with the decrease of Ni^{2+}, leading to the rise on pH value for the reaction solution. As a result, the reaction of Ni^{2+} with BH_4^- was inhibited and then decreased Ni/W mole ratio on the catalyst surface. On the other hand, the formation of complex hindered the precipitation reaction between Ni^{2+} and OH^- to produce $Ni(OH)_2$, causing the increasing Ni^0 content and decreasing $Ni(OH)_2$ on the catalyst surface. Table 1 showed that Ni^0 content on the catalyst surface in this study was much higher than that in the previous study [18]. This suggested that adding $NH_3 \cdot H_2O$ was beneficial to improve the Ni^0 content on the catalyst surface, but adding exceeding $NH_3 \cdot H_2O$ lowered the total of Ni content.

As shown in Fig. 2, all the samples displayed only one broad peak centered at $2\theta = 45°$, presenting a typical amorphous structure [19–21]. The intensity of this peak ($2\theta = 45°$) corresponded to amorphous degree [22]. Ni–W-2 exhibited a weaker peak than Ni–W-1, indicating the higher amorphous degree of Ni–W-2 and the lower amorphous degree of Ni–W-1. It had reported that tungsten oxides and phosphorus oxide could act as dispersant agents [20,24]. Hence, W^{6+} and P^{n+} species could prevent the particle agglomeration efficiently, resulting in the high amorphous degree. On the contrary, there existed a strong interaction between Ni^0 and B^0 and Ni^0 and P^0 in the prepared catalysts, leading to the promoted agglomeration of particles. The more the B^0 and P^0 contents on the catalyst surface are, the lower the amorphous degree. The surface area results also supported this inference. As shown in Table 1, the surface area decreased in the order of Ni–W-0.5 (28.0 m^2/g) > Ni–W-2 (24.5 m^2/g) > Ni–W-0.33 (22.4 m^2/g) > Ni–W-1 (17.2 m^2/g). In addition, the XPS results demonstrated that the prepared catalysts contained W^0, W^{6+}, P and P^{n+}, but these species were not observed in Fig. 2, indicating that these species were in amorphous state and dispersed evenly in the catalyst.

3.2. Hydrodeoxygenation of p-cresol on Ni–W–P–B catalysts

The conversion and product selectivity versus reaction time in the HDO of *p*-cresol on Ni–W-1 at 498 K are shown in Fig. 3a. Methylcyclohexane, 3-methylcyclohexene, toluene, 4-methylcyclohexanol and 4-methylcyclohexanone were produced during *p*-cresol HDO reaction. After 1 h, the conversion reached to 99.6% with a selectivity of 51.1% 4-methylcyclohexanol. Then, the HDO reaction in this system was changed to the HDO of 4-methylcyclohexanol. The selectivity of methylcyclohexane increased to 92.6% while the selectivity of toluene increased to 5.1% for 5 h. Hence, it was concluded that the main reaction route was HYD, where 4-methylcyclohexanone and 4-methylcyclohexanol acted as intermediates. The toluene selectivity increased from 2.1% to 5.1% in the following 4 h. However, according to

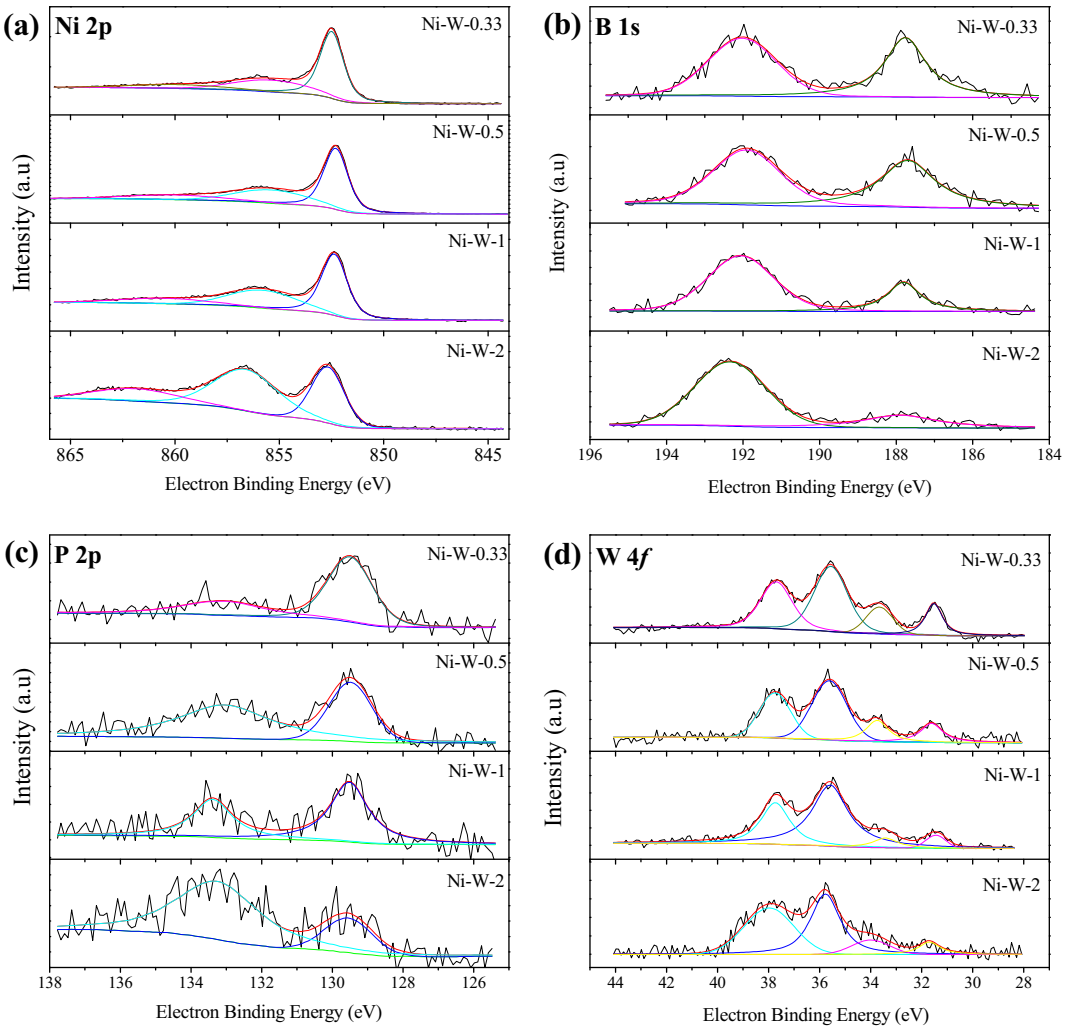

Fig. 1. XP spectra of (a) Ni 2p, (b) B 1s, (c) P 2p and (d) W 4f of Ni–W–P–B samples.

DDO route, this increase of toluene via the direct C–O bond scission was impossible because there remained only 0.4% *p*-cresol in the reactor, which might be derived from *4*-methylcyclohexanol. To verify this hypothesis, we studied the HDO of *4*-methylcyclohexanol on Ni–W-1 amorphous catalyst under the same conditions. The results were showed in Fig. 3b. At the end, the selectivity of *4*-methylcyclohexanone and toluene was 3.8% and 11.6%, respectively. This suggested that there exists a dehydrogenation reaction. *4*-Methylcyclohexanone was yielded by the dehydrogenation of *4*-methylcyclohexanol while toluene was generated from the dehydrogenation of *3*-methylcyclohexene, as shown in Scheme 1. According to the HDO of *4*-methylcyclohexanol, the DDO route in the HDO of *p*-cresol might not occur at 498 K because the direct scission of *C–O* bond in phenols needs a high activation energy. Moreover, our previous study [18] had also found that Ni–W–B amorphous catalyst had no DDO activity at 498 K. Therefore, it can be concluded that Ni–W–P–B amorphous catalyst possesses HDO activity and dehydrogenation activity simultaneously.

The conversion and product distribution in the HDO of *p*-cresol on Ni–W-2, Ni–W-1, Ni–W-0.5 and Ni–W-0.33 at 498 K for 5 h are showed in Table 2. *p*-Cresol conversion increased firstly and then decreased, while toluene selectivity increased with Ni/W mole ratio. Ni–W-1 exhibited the highest HDO activity: conversion was up to 100% with a deoxygenation degree of 100% and a selectivity of 5.1% toluene. This indicated that the catalyst with an appropriate Ni/W mole ratio enhanced the HDO activity and increasing W content promoted dehydrogenation activity. This was mainly attributed to the composition on the catalyst surface. For the conversion, Ni–W–P–B amorphous catalyst had high Ni^0, B^0 and P^0 contents and electron transfer, leading to its high hydrogenation activity, which made the HDO of *p*-cresol proceeded with HYD route [25]. Low total content of Ni^0 contributed to the low

Table 1
Surface area and surface composition of Ni–-W–-P–-B catalysts.

Catalysts	S_{BET} (m^2/g)	Surface composition	Ni (%)		B (%)		P (%)		W (%)	
			Ni^0	Ni^{2+}	B^0	B^{3+}	P^0	P^{n+}	W^0	W^{6+}
Ni–W-2	24.5	$Ni_{1.00}W_{0.22}B_{3.55}P_{0.35}$	33.1	66.9	22.5	77.5	20.4	79.6	16.6	83.4
Ni–W-1	17.2	$Ni_{1.00}W_{0.82}B_{2.02}P_{0.45}$	52.2	47.8	26.4	73.6	60.1	39.9	10.9	89.1
Ni–W-0.5	28.0	$Ni_{1.00}W_{1.22}B_{3.87}P_{0.64}$	55.4	44.6	48.0	52.0	36.6	63.4	26.6	73.4
Ni–W-0.33	22.4	$Ni_{1.00}W_{4.36}B_{8.01}P_{1.18}$	60.2	39.8	47.4	52.6	68.1	31.9	29.2	70.8

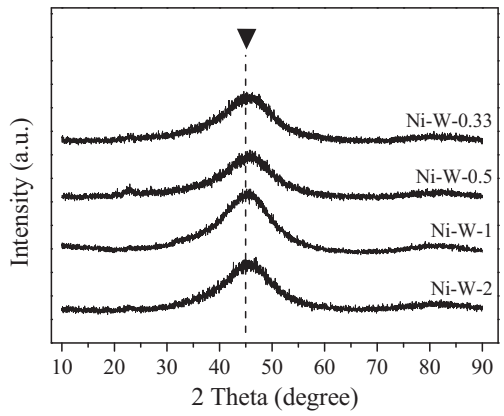

Fig. 2. XRD patterns of Ni–W-2, Ni–W-1, Ni–W-0.5 and Ni–W-0.33.

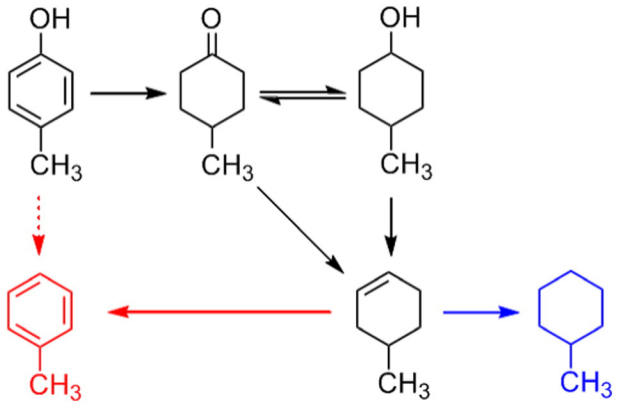

Scheme 1. Proposed reaction routes for the HDO of *p*-cresol on Ni–W–P–B amorphous catalyst.

conversion. For example, the conversion on Ni–W-1 with a surface composition of $Ni_{1.00}W_{0.82}B_{2.02}P_{0.45}$ was 100%, but it decreased to 93.2% on Ni–W-0.33 with a surface composition of $Ni_{1.00}W_{4.36}B_{8.01}P_{1.18}$, as shown in Tables 1 and 2. This HYD route avoided the direct deoxygenation, which could reduce the HDO reaction temperature and aromatic content in the product. Deoxygenation reaction required two kinds of active sites: metal site and Brönsted acid site [26]. The product distribution was closely related to the balance between these two sites [27]. The characterization results had displayed that W in Ni–W–P–B catalysts existed in the form of WO_3. This W oxide had Brönsted acidity [28]. Moreover, unreduced phosphorus also increased the Brönsted acid sites on the catalyst surface [24]. Although the Brönsted acid sites increased, the total metal sites on catalyst surface reduced with W content, leading to the high toluene selectivity and low *4*-methylcyclohexanol selectivity. Scheme 1 indicated that toluene was generated from the dehydrogenation of 3-methylcyclohexene. The relation between the characterization and HDO activity results seems to mean that the toluene selectivity depends on the W content on the catalyst surface, but which needs to be further studied.

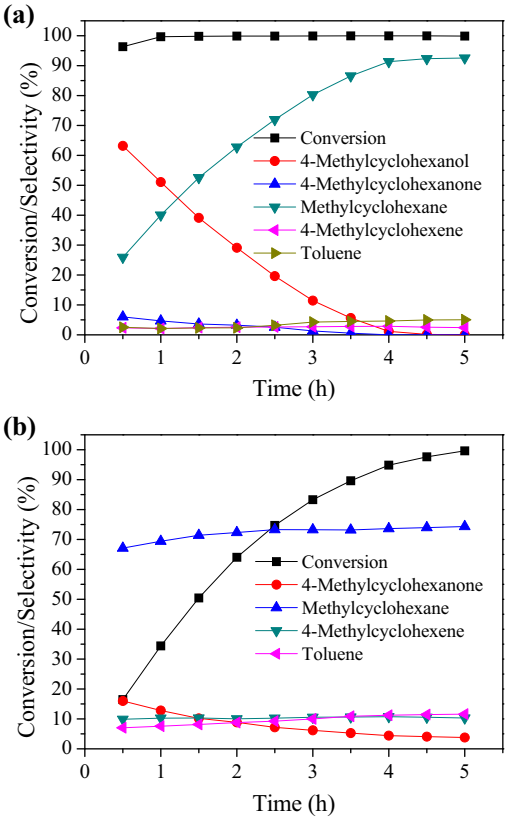

Fig. 3. HDO of (a) *p*-cresol and (b) *4*-methylcyclohexanol on Ni–W-1 at 498 K.

4. Conclusion

When adding $NH_3 \cdot H_2O$ during the preparation of Ni–W–P–B amorphous catalyst, the alone Ni^{2+} concentration decreased and the reaction rate of Ni^{2+} with BH_4^- was inhibited because of a formation of complex between Ni^{2+} and $NH_3 \cdot H_2O$, promoting the reduction of Ni^{2+} to Ni^0, which yielded a high Ni^0 content on the catalyst surface. P in the catalyst existed in the form of P^0 and P^{n+}, the former state could enhance the hydrogenation while the latter state acted as Brönsted acid sites. Ni–W–P–B amorphous catalyst exhibited high activity in the HDO of *p*-cresol. The deoxygenation degree was high to 100% with a toluene selectivity of 5.1% at 498 K. Both the HDO reaction temperature and aromatic yield decreased obviously. Ni–W–P–B also possessed a dehydrogenation activity.

Acknowledgments

This work was supported by Natural Science Foundation of Hunan Province (13JJ4048), National Natural Science Foundation of China (no. 21306159, 21376202) and Specialized Research Fund for the Doctoral Program of Higher Education (20124301120009).

Table 2
Comparison of the HDO of *p*-cresol on Ni–W-2, Ni–W-1, Ni–W-0.5 and Ni–W-0.33 at 498 K for 5 h.

Catalysts	Ni–W-2	Ni–W-1	Ni–W-0.5	Ni–W-0.33
Conversion, mol%	98.1	100	99.7	93.2
Product distribution, mol%				
4-Methylcyclohexanol	28.8	0	9.3	18
4-Methylcyclohexanone	2.3	0	2.9	7.6
3-Methylcyclohexene	4.2	2.4	12.2	0.6
Methylcyclohexane	59.8	92.5	62.6	56.5
Toluene	4.9	5.1	13	17.3
DD, wt.%	67.5	100	89.2	72.6

References

[1] J.C. Serrano-Ruiz, J.A. Dumesic, Energy Environ. Sci. 4 (2011) 83–99.
[2] H. de Lasa, E. Salaices, J. Mazumder, R. Lucky, Chem. Rev. 111 (2011) 5404–5433.
[3] P. Azadi, O.R. Inderwildi, R. Farnood, D.A. King, Renew. Sust. Energ. Rev. 21 (2013) 506–523.
[4] H. Wang, J. Male, Y. Wang, ACS Catal. (2013) 1047–1070.
[5] W. Wang, K. Zhang, Z. Qiao, L. Li, P. Liu, Y. Yang, Ind. Eng. Chem. Res. 53 (2014) 10301–10309.
[6] G. Veryasov, M. Grilc, B. Likozar, A. Jesih, Catal. Commun. 46 (2014) 183–186.
[7] T.A. Le, H.V. Ly, J. Kim, S.-S. Kim, J.H. Choi, H.-C. Woo, M.R. Othman, Chem. Eng. J. 250 (2014) 157–163.
[8] A. Iino, A. Cho, A. Takagaki, R. Kikuchi, S. Ted Oyama, J. Catal. 311 (2014) 17–27.
[9] Y.-K. Hong, D.-W. Lee, H.-J. Eom, K.-Y. Lee, Appl. Catal. B Environ. 150–151 (2014) 438–445.
[10] S. Boullosa-Eiras, R. Lødeng, H. Bergem, M. Stöcker, L. Hannevold, E.A. Blekkan, Catal. Today 223 (2014) 44–53.
[11] W. Wang, K. Zhang, Y. Yang, H. Liu, Z. Qiao, H. Luo, Microporous Mesoporous Mater. 193 (2014) 47–53.
[12] J.-S. Moon, E.-G. Kim, Y.-K. Lee, J. Catal. 311 (2014) 144–152.
[13] M.S. Zanuttini, C.D. Lago, C.A. Querini, M.A. Peralta, Catal. Today 213 (2013) 9–17.
[14] Y.Q. Yang, C.T. Tye, K.J. Smith, Catal. Commun. 9 (2008) 1364–1368.
[15] C. Wang, D. Wang, Z. Wu, Z. Wang, C. Tang, P. Zhou, Appl. Catal. A Gen. 476 (2014) 61–67.
[16] Y. Yang, A. Gilbert, C. Xu, Appl. Catal. A Gen. 360 (2009) 242–249.
[17] W. Wang, K. Zhang, H. Liu, Z. Qiao, Y. Yang, K. Ren, Catal. Commun. 41 (2013) 41–46.
[18] W. Wang, Y. Yang, H. Luo, H. Peng, F. Wang, Ind. Eng. Chem. Res. 50 (2011) 10936–10942.
[19] H. Li, Q. Zhao, H. Li, J. Mol. Catal. A Chem. 285 (2008) 29–35.
[20] B. Zhao, C.J. Chou, Y.W. Chen, Ind. Eng. Chem. Res. 49 (2010) 1669–1676.
[21] H. Li, H. Li, J. Deng, Catal. Today 74 (2002) 53–63.
[22] W.J. Wang, J.H. Shen, Y.W. Chen, Ind. Eng. Chem. Res. 45 (2006) 8860–8865.
[23] S.P. Lee, Y.W. Chen, Ind. Eng. Chem. Res. 38 (1999) 2548–2556.
[24] J.A. Cecilia, A. Infantes-Molina, E. Rodríguez-Castellón, A. Jiménez-López, S.T. Oyama, Appl. Catal. B Environ. 136–137 (2013) 140–149.
[25] H. Li, Y. Wu, H. Luo, M. Wang, Y. Xu, J. Catal. 214 (2003) 15–25.
[26] N. Yan, Y. Yuan, R. Dykeman, Y. Kou, P.J. Dyson, Angew. Chem. Int. Ed. 49 (2010) 5549–5553.
[27] F.E. Massoth, P. Politzer, M.C. Concha, J.S. Murray, J. Jakowski, J. Simons, J. Phys. Chem. B 110 (2006) 14283–14291.
[28] G. Lu, X. Li, Z. Qu, Q. Zhao, H. Li, Y. Shen, G. Chen, Chem. Eng. J. 159 (2010) 242–246.